KTH Engineering Sciences

Characterisation of anisotropic acoustic properties of porous materials - inverse estimation of static flow resistivity

Christophe Van der Kelen

Licentiate Thesis

Stockholm, March 2011
The Marcus Wallenberg Laboratory of Sound and Vibration Research
Department of Aeronautical and Vehicle Engineering
Kungliga Tekniska Högskolan

Postal address
Royal Institute of Technology
MWL / AVE
SE-100 44 Stockholm
Sweden

Visiting address
Teknikringen 8
Stockholm

Contact
Tel: +46 8 790 64 41
Email: cjfvdk@kth.se

Akademisk avhandling som med tillstånd av Kungliga Tekniska Högskolan i Stockholm framläggs till offentlig granskning för avläggande av teknologie licentiatexamen tisdag den 15 mars 2011, 10:00 i sal MWL74, Teknikringen 8, KTH, Stockholm.

TRITA-AVE-2011:14
ISSN-1651-7660
ISBN-978-91-7415-894-6

Pour a bottle of beer. Restraining your thirst for the moment, admire its lively performance. One by one, bubbles of gas are nucleated, rise and crowd together at the surface. A foam, or froth, is quickly formed. Most of the liquid drains away, leaving the bubbles packed closely together in the form of elegant polyhedral cells. If you wait long enough you may see the structure change, as gas diffuses between the cells. This gradual change is punctuated by sudden local rearrangements. In most brands of beer it is quickly overtaken by the collapse of the foam, as its individual films burst. Drink it in time, and you can feel that the foam is not quite a liquid. Paradoxically, it is a very soft solid, creamy in texture if the bubbles are small. Cheers!

D. Weaire and S. Hutzler, The physics of foams (2001), Oxford University Press, page 1

Abstract

The production processes of porous materials introduce an inherent geometric anisotropy in the material at micro scale, which influences the material properties at macro scale. In this thesis, the focus is turned to one of these macroscopic properties, the flow resistivity, which is a measure of the resistance felt by the sound pressure waves as they propagate through a porous space. In the current work, two different porous materials have been studied, a fibrous glass wool and a Melamine foam. The two materials are expected to show different degrees of anisotropy with respect to flow resistivity. Glass wool is assumed to be transversely isotropic, as a result of the stacking of layers of fibres. The level of anisotropy in Melamine foam is not as obvious, and might be related to production specific aspects, such as the rise-direction, and the position of the injection nozzles. The thesis begins by giving an introduction to porous materials in general, and to glass wool and Melamine foam in particular, followed by an introduction to flow resistivity, together with two methods to measure the flow resistivity. The full anisotropic flow resistivity of glass wool and Melamine foam samples is determined by means of measurements and inverse estimation. An eigenvalue and eigenvector decomposition of the flow resistivity tensor provides an insight into the connection between the directionality of the flow resistivity in each material, and its production process. A study of the homogeneity in density and flow resistivity for the two materials shows that these properties vary within the block of material. However, for each material, there seems to be no connection between the variation in the two properties, investigated at the macroscopic scale.

Dissertation

A Licentiate of Technology is an intermediate Swedish academic degree that can be obtained half-way between the MSc and the PhD. While less formal than a Doctoral Dissertation, examination for the degree includes writing a thesis and a public presentation.

The work presented in this Licentiate was carried out within the Marcus Wallenberg Laboratory for Sound and Vibration Research at the Department of Aeronautical and Vehicle Engineering, the Royal Institute of Technology (KTH) in Stockholm, Sweden.

This thesis consists of two parts. The first part gives an overview of the research with a summary of the performed work. The second part collects the following scientific articles:

Paper A. C. Van der Kelen and P. Göransson, *Measurement and Inverse Estimation of the Full Anisotropic Flow Resistivity Tensor of Melamine Foam.* To be submitted.

Paper B. C. Van der Kelen, P. Göransson and N.E. Hörlin, *Measurement and Inverse Estimation of the Full Anisotropic Flow Resistivity Tensor of Glass Wool.* To be submitted.

Division of Work Between the Authors

Paper A. Van der Kelen worked on the improvements discussed for the method, performed the measurements, simulations, and post-processing analysis, and wrote the paper under the supervision of Göransson.

Paper B. Van der Kelen and Hörlin developed the mathematical derivation. Van der Kelen performed the measurements, simulations, and post-processing analysis, and wrote the paper under the supervision of Göransson.

Acknowledgements

I would like to thank my advisor, Professor Peter Göransson, who has been a huge help in writing this thesis, guiding me through the process from student to adult, both in research and life, and keeping me with my feet on the ground by showing me that there is still a lot to be learned. I also thank him for his patience, and his help in times of high needs, such as the past three months.

The study presented in this thesis has been carried out at the Marcus Wallenberg Laboratory of Sound and Vibration research (MWL), KTH. The research was funded with the support from the European Union, the Smart Structures project (Contract no. MRTN-CT-2006-035559), which is gratefully acknowledged.

The provision of glass wool by Ecophon® and Melamine foam by my late Professor Walter Lauriks is thankfully acknowledged.

A great part of my life at KTH is occupied by BEST Stockholm, through which I have had the opportunity to meet a lot of people, and to live experiences that will without doubt prove most valuable in later life. The enthusiasm of the people I may work with in my free time gives me a smile on my face, and makes me continue every day.

To Professor Fülöp Augusztinovicz, who invited me to work at the Budapest University of Technology and Economics (BME), where I met friends for life in a magnificent city.

To my colleagues at the department for keeping me fit by weekly movement, and for revising this thesis, and helping me with comments, as I sometimes got lost in the writing.

The staff members of MWL have helped a lot in the course of the work. Thank you Dr Kent Lindgren and Mr Danilo Prevelić, who helped me a lot from the moment I arrived in KTH in 2007. It is my great pleasure to work with the people of the MWL Laboratory.

I think my parents deserve the thank you since they were always supportive, and my gratitude towards them can not be expressed in words only. Without them and their unconditional support I would not have been where I am today.

Contents

Chapter 1

Introduction

1.1 Background

Porous materials are interesting from an acoustical point of view for the transportation industry, automotive, aeronautical, rail, etc., as such materials can meet the conflicting requirements the industry is facing. On the one hand there are the economic and ecologic demands driven by the need for reduced fuel consumption, and reduced environmental impact in the life-cycle of a transportation vehicle. On the other hand there are the demands on quality and comfort such as noise, vibration, safety and reliability.

The choice of a particular material is often defined by a trade off between these conflicting requirements. As an example, the weight is currently a primary issue for most engineering systems that are parts of the everyday mobility of humans and goods. However, by using lightweight materials to reduce the weight, the vibration and noise levels inevitably increase. This increase can be limited by tailoring the used materials, and by optimising their performance for specific applications.

The ability to adapt a porous material to specific applications, is one of the most significant potential advantages of a porous material over an ordinary solid material. Porous materials, such as foams, are materials with inherent design parameters, available at the microscopic level, which have a significant impact on the macroscopic properties, and thus the mechanical and thermal behaviour. In order to obtain a material with parameters optimised for specific applications, the following chain needs to be studied (and ultimately linked): *Foam chemistry - Foam processing - Foam cell micromechanics - Macroscopic static & dynamic properties - End application performance*.

The work in this thesis is part of the development of a non-destructive testing methodology, where one sample can be used to estimate the macroscopic static and dynamic properties of a porous material, such as the static flow resistivity, and the elastic and dynamic

moduli. The focus is here on the measurement and inverse estimation of the anisotropic flow resistivity tensor in porous materials. Two materials are investigated: fibrous glass wool and Melamine foam. Fibrous glass wool is interesting due to its inherent transverse isotropy, while the highly porous, open-celled Melamine foam is very interesting from acoustical point of view, and its (anisotropic) properties are as yet not very well known. [1, 8, 10]

1.2 Scope of the thesis

In chapter 2, an introduction to porous materials is given, and the two materials examined in this study (Melamine foam and glass wool) are shown to have particular properties as a result of the production process. In chapter 3, the term flow resistivity is introduced together with the terminology related to the flow resistivity in porous materials. Moreover, two methods for the measurement of flow resistivity are described. One is the International Standard ISO 9053 [11], the other is an alternative method recently proposed by Göransson et al. [9]. Chapters 2 and 3 provide background information to give a better understanding, when discussing the identified flow resistivity in Melamine foam and glass wool in chapter 4.

In paper **A**, the measurement method is further improved and verified, and the anisotropic flow resistivity tensor is identified of seven Melamine foams from two different foam blocks.
In paper **B**, the anisotropic flow resistivity tensor of nine glass wool samples of one slab of glass wool is identified, and a comparison is made between the variation in density and flow resistivity through the material.

Chapter 2

Introduction to porous materials

The world today would be hard to imagine without porous materials. Mankind has used them during many thousands of years, and today we even eat and drink them. Several stones are porous materials. Bread, beer, cereals, snacks, honey, they are all edible porous materials. Sponges, cushions, cork, wood, coffee cups are porous materials we use everyday. Moreover, during the last century, we have learned to produce industrial foams ourselves for application as thermal and acoustical insulation.

2.1 What is a porous material?

A porous material is characterised by having two or more phases, where one of them is a connected space, forming a network of cells that are filled with a fluid. In a solid porous material, the edges and faces of the cells that contain the fluid, are made of solid material. Solid porous materials can be 100 times lighter than the material of which it is produced [20], and this makes them very interesting for lightweight constructions. Depending on the structure of the solid frame, porous media typically belong to one of the following categories (see Figure 2.1) [1, 7]:

- Porous materials with two-dimensional networks, also called *honeycombs*, with important applications in the construction of lightweight structures (see Figure 2.1a). [7]
- Porous materials with three-dimensional networks. These can be divided into
  - *Fibrous materials*
    Generally formed by thin (0.1 - 20 μm) natural or synthetic fibres. The material normally consists of stacked layers, in which the fibres are randomly oriented. This causes a characteristic anisotropy, and a different mechanical, thermal and acoustical performance in directions parallel and perpendicular to the stacking direction (see Figure 2.1b). [1]

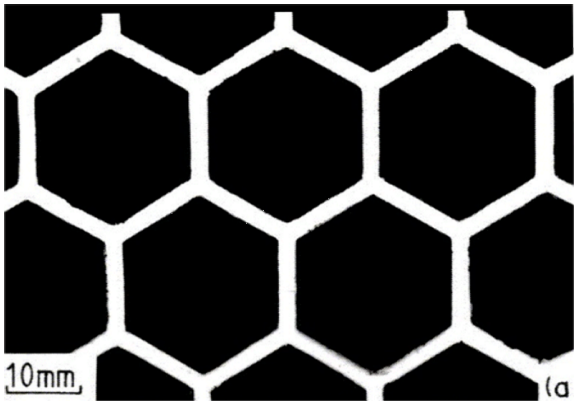

(a) Honeycomb (Gibson and Ashby [7])

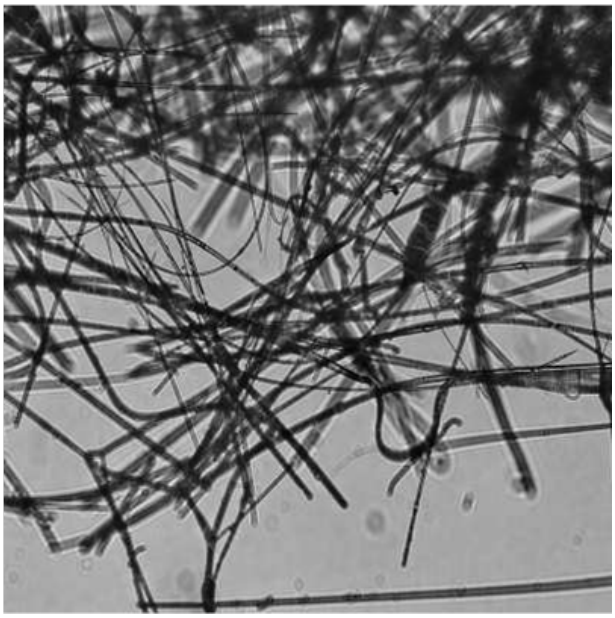

(b) Glass wool (Guastavino [10])

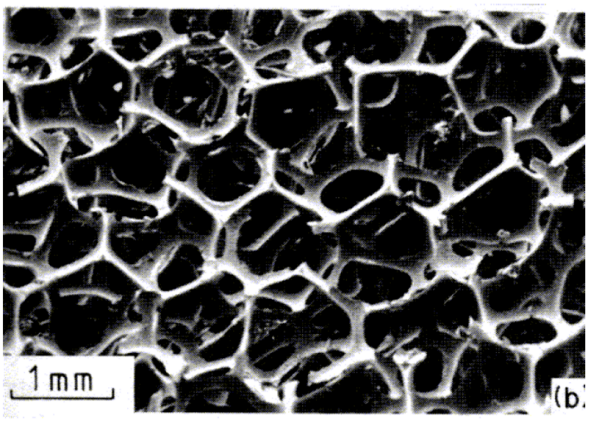

(c) Open-cell foam (Gibson and Ashby [7])

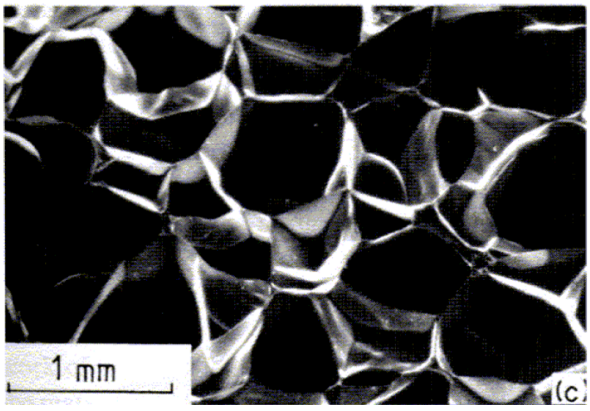

(d) Closed-cell foam (Gibson and Ashby [7])

Figure 2.1: Different types of porous structures.

– *Foams*
Two kinds of foam exist: open-celled foam (see Figure 2.1c), where the solid material is contained in the cell edges only (so the cells connect through open faces), and closed-celled foam (see Figure 2.1d), which has solid cell edges and faces, so that each cell is sealed of from its neighbours. Some foams can be partly open and partly closed. [7]

The porosity ϕ is an important property of porous materials. It is equal to the ratio of the air volume V_a to the total volume V_T of the porous material [2]:

$$\phi = \frac{V_a}{V_T}. \tag{2.1}$$

If V_b is the volume occupied by the solid material in V_T, the quantities V_a, V_b and V_T are related by

$$V_a + V_b = V_T. \tag{2.2}$$

In this thesis, the materials under investigation are glass wool and Melamine foam. Glass wool is a fibrous material, and Melamine foam is an open-cell foam. Both materials are very light, and have a porosity of approximately 0.99, which means that 99% of the total volume of the material is air. Nevertheless, as will be shown, the acoustic properties of glass wool and Melamine foam are quite different.

2.2 Applications and production of porous materials

This section describes briefly the application area and the production process of glass wool and Melamine foam. The production process introduces an inherent geometric anisotropy at micro scale, which influences the material properties at macro scale. A closer look at the production process of the material can help to give a better understanding of their geometric properties at micro scale, when discussing the flow resistivity of these materials in chapter 4 .

2.2.1 Glass wool

Glass wool is an insulating material made from fibreglass. It is characterised by its low weight, good fire protection, good thermal insulation and sound-absorption performance. Therefore it is used in a wide range of applications such as thermal and/or acoustical insulation for buildings, tanks, boilers, turbines, offshore installations, ships and aircraft. [18]

Figure 2.2 shows the production process of glass wool. The required amounts of raw material are sent to a melting furnace. For glass wool the raw materials are sand, limestone and soda ash, as well as recycled cuts from the production process. The raw materials are melted in a furnace at temperatures up to 1500°C. After the furnace, droplets of the vitreous melt are shaped into fibres, and small quantities of binding agents are added to the fibres. The structure and density of the product can now be adapted to

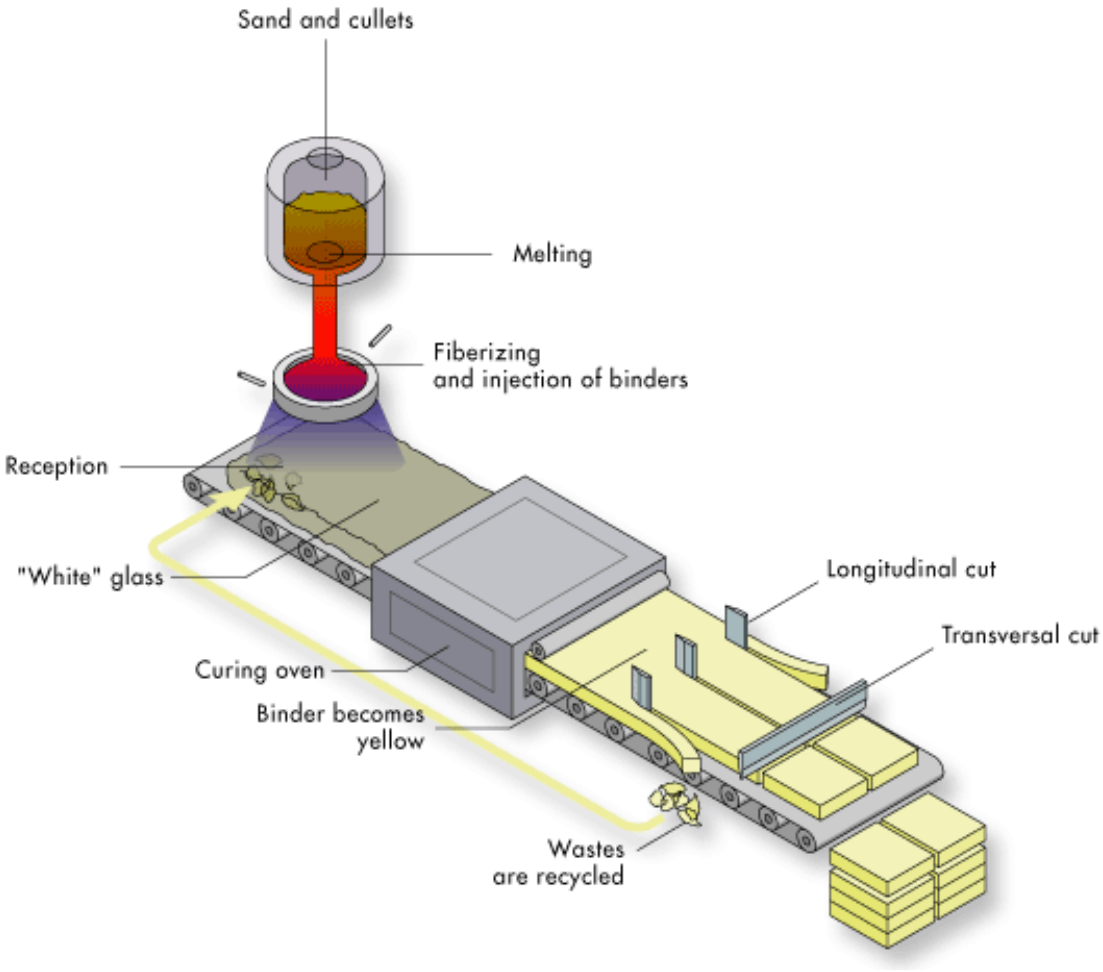

Figure 2.2: Visual representation of the production process of glass wool (EURIMA [18]).

its precise final usage. The material is then cured at around 200°C, and the glass wool is finally sawn to the required size and shape. [18]

Once the glass wool fibres are shaped, they fall on the conveyor belt, and are arranged into a texture existing of layers, in which the fibres are randomly oriented (see Figure 2.1b). These layers are resting on each other, connected by a binder, and as such form a stack. This layered structure causes a characteristic anisotropy in the material, and the properties in the plane parallel to the layers (in planar or in-plane direction) are expected to be different from the properties perpendicular to the layers (in stacking or out-of-plane direction).

2.2.2 Melamine foam

Melamine is a flexible, open-cell foam made from Melamine resin, a thermoset polymer. Its characteristic feature is a three-dimensional network structure, consisting of slender webs (see Figure 2.3). Melamine is characterised by its low weight, good sound-absorption capacity, good thermal insulation properties, flame resistance and abrasiveness. It is used for cleaning, as insulation in construction, and as insulation and seating in transportation. [17]

As many foams, Melamine is manufactured by injection moulding. An aqueous solution or dispersion which contains a melamine/formaldehyde mixture, an emulsifier, a foaming agent[1], and a curing agent, is injected through a nozzle and immediately foamed by heating to a temperature above the boiling point of the foaming agent. Depending on the foaming process, a foam block or strand is obtained, which is cured by annealing[2], to give the final product. [4, 13]

In injection moulding, the aqueous solution is injected into a foaming chamber. During the foaming process, the geometry of the cells and the dimensions of the struts are influenced by the rise and injection-flow directions, elongating the cells by the effect of gravity [10]. The rise and injection-flow directions will have an important influence on the properties of the foam, as it introduces a characteristic anisotropy in the material. Their influence is visible in the microstructure of the foam, as shown in Figure 2.3.

[1] "Any substance which alone or in combination with other substances is capable or producing a cellular structure in a plastic mass." [19]

[2] "The process of relieving internal stresses of molded plastic articles by heating to a predetermined temperature, maintaining this temperature for a predetermined length of time, and slowly cooling the articles." [19]

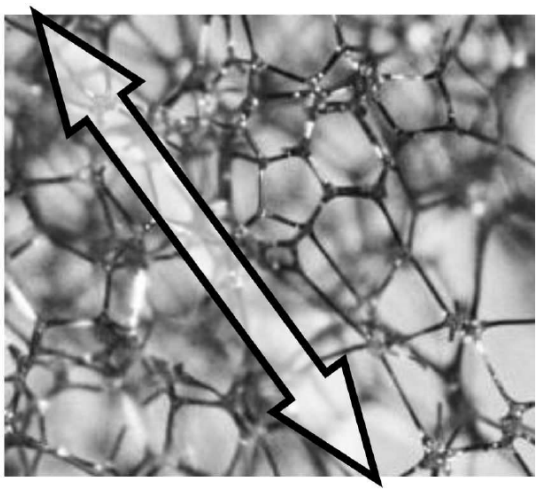

Figure 2.3: Microscopic photography of Melamine foam with possible principle direction of cell orientation (Guastavino [10]).

Chapter 3

Flow resistivity in porous materials

When porous materials are used for vibro-acoustic purposes, the flow resistivity is one of the properties used to characterise the behaviour on macro scale of a certain micro-structural geometry. It provides an accumulated measure for the viscous drag losses occurring at micro scale, and is used in the modelling on macro scale.

3.1 Introduction to flow resistivity

The static air-flow resistivity $\boldsymbol{\sigma}$ is an important parameter used to describe the acoustical behaviour of porous materials. It has been used from the beginning to predict the acoustical properties of acoustic materials. It indicates to what extent a material offers resistance to a fluid that flows through the material.

3.1.1 Definition

In one dimension, flow resistivity is defined as the ratio of the static pressure drop across a sample of material, to the normal flow velocity through the material. A sketch of the traditional set-up for the measurement of flow resistivity is shown in Figure 3.1. The material is placed in a pipe, and a pressure difference across the material induces a steady flow of air. The flow resistivity σ_{1D} is given by

$$\sigma_{1D} = -\frac{p_2 - p_1}{V \cdot t} \tag{3.1}$$

where V is the mean flow of air per unit area of the material, and t is the thickness of the material sample. A negative sign in the right side of the equation has to be added since a positive air flow is from higher pressure p_1 to lower pressure p_2. [2]

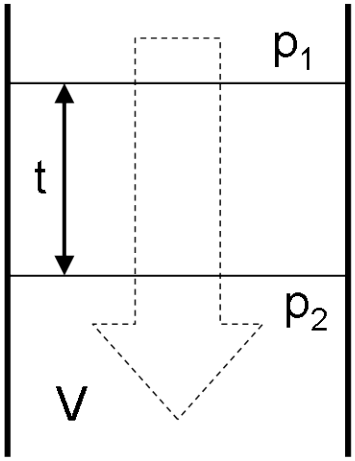

Figure 3.1: A slice of porous material in a pipe. A differential pressure $p_1 - p_2$ induces a steady air-flow V or air per unit area of material. [2]

In 3D, the flow resistivity can be represented by a symmetric tensor ($\sigma_{ij} = \sigma_{ji}$), defined by Darcy's law [6]:

$$\begin{bmatrix} \frac{\partial p}{\partial x} \\ \frac{\partial p}{\partial y} \\ \frac{\partial p}{\partial z} \end{bmatrix} = - \begin{bmatrix} \sigma_{xx} & \sigma_{xy} & \sigma_{xz} \\ & \sigma_{yy} & \sigma_{yz} \\ sym & & \sigma_{zz} \end{bmatrix} \begin{bmatrix} u_x \\ u_y \\ u_z \end{bmatrix} \tag{3.2}$$

To understand the influence of the terms in Eq.(3.2), a 2D simplification of Darcy's law may be helpful:

$$\begin{bmatrix} \frac{\partial p}{\partial x} \\ \frac{\partial p}{\partial y} \end{bmatrix} = - \begin{bmatrix} \sigma_{xx} & \sigma_{xy} \\ \sigma_{yx} & \sigma_{yy} \end{bmatrix} \begin{bmatrix} u_x \\ u_y \end{bmatrix} \tag{3.3}$$

Figure 3.2 represents a sample of material with a length l and thickness t, for which $l >> t$. In this case it is valid to assume that $u_y = 0$. A steady air flow is introduced in the sample with a constant velocity $u_x = V$. Then the following equations are valid:

$$\frac{\partial p}{\partial x} = -\sigma_{xx} \cdot u_x, \tag{3.4}$$

$$\frac{\partial p}{\partial y} = -\sigma_{xy} \cdot u_x. \tag{3.5}$$

The term σ_{xx} induces a pressure difference parallel to the x axis, defined by Eq.(3.4), which is essentially the same as Eq.(3.1). The term σ_{xy} induces a pressure difference parallel to the y axis, although the velocity parallel to the y axis (u_y) is equal to zero.

Figure 3.2: A slice of porous material in a 2D representation.

3.1.2 Terminology related to flow resistivity in porous materials

In chapter 2, it was pointed out that the production processes of glass wool and Melamine foam are introducing a characteristic anisotropy in the material. Terms related to homogeneity and isotropy are frequently used, when discussing flow resistivity in porous materials. Therefore, they will be briefly explained here.

Homogeneous and inhomogeneous materials

In reference [12], page 10, a definition for both terms is given:

- "A *homogeneous* body has uniform properties throughout, i.e., the properties are not a function of *position* in the body."
- "An *inhomogeneous* body has non-uniform properties over the body, i.e., the properties are a function of *position* in the body."

In the present work, the spatial variation of the flow resistivity is always assumed to be small on the scale of the sample size. Results from measurements suggest, however, that this assumption is not valid on the scale of the entire block of material, as there appears to be a variation in flow resistivity between adjacent samples [5, 16].

Isotropy and anisotropy in porous materials

In reference [12], page 10, the following definitions can be found:

- "An *isotropic* body has material properties that are the same in every direction at a point of the body, i.e., the properties are not a function of *orientation* at a point in the body."
  In an isotropic material, the flow resistivity tensor is always

$$\boldsymbol{\sigma} = \begin{bmatrix} \sigma_1 & 0 & 0 \\ & \sigma_1 & 0 \\ sym & & \sigma_1 \end{bmatrix}, \tag{3.6}$$

  which means that knowledge of one value, σ_1, is sufficient to describe the flow resistivity in the material.

- "An *orthotropic* body has material properties that are different in three mutually perpendicular directions [(or principal directions)] at a point in the body and, further, have three mutually perpendicular planes of material symmetry. Thus, the properties are a function of *orientation* at a point in the body."
  In an orthotropic material, it is always possible to write the flow resistivity tensor as (if necessary with some transformations)

$$\boldsymbol{\sigma} = \begin{bmatrix} \sigma_1 & 0 & 0 \\ & \sigma_2 & 0 \\ sym & & \sigma_3 \end{bmatrix}, \tag{3.7}$$

  which means that there are three principal directions in the material along which the flow resistivity is described by a one value, the principal value. For a random direction, the flow resistivity will depend on all three values σ_1, σ_2 and σ_3.

  A special case of orthotropy is *transverse isotropy*. "If at every point of a material there is one plane in which the mechanical properties are equal in all directions, then the material is termed *transversely isotropic*", ([12] page 35). In a transversely isotropic material, it is always possible to write the flow resistivity tensor as (if necessary with some transformations)

$$\boldsymbol{\sigma} = \begin{bmatrix} \sigma_1 & 0 & 0 \\ & \sigma_1 & 0 \\ sym & & \sigma_3 \end{bmatrix}, \tag{3.8}$$

  or a special case of orthotropy with $\sigma_1 = \sigma_2$.

In this thesis, an *anisotropic* body will be the general name for all bodies which are not isotropic, i.e., when the flow resistivity in the material is dependent on the orientation. Transverse isotropy and orthotropy are hence two special cases of anisotropy.

3.2 Measurement of flow resistivity in porous materials

The purpose of this work is to determine the flow resistivity in porous materials. The most straightforward method to measure flow resistivity is standardised in the International Standard ISO 9053: "The Measurement of Flow Resistance in Porous Acoustic Materials", [11].

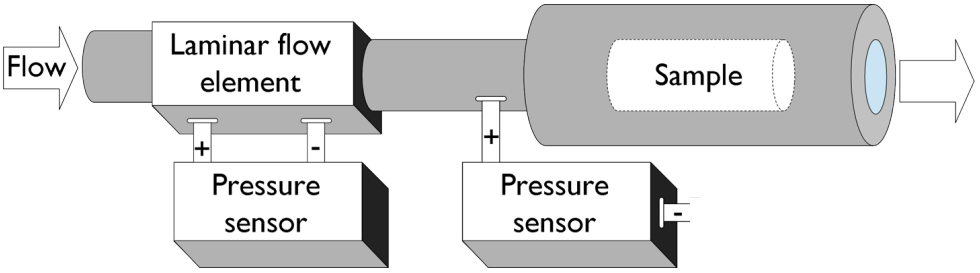

Figure 3.3: General arrangement of measurement set-up according to ISO 9053.

3.2.1 Measurement method according to the International Standard ISO 9053

In this section, the International Standard ISO 9053 [11] is described, together with some observations, showing the need for a more accurate method to estimate the flow resistivity of porous materials.

Figure 3.3 presents a general arrangement of the measurement set-up described in the International Standard ISO 9053 [11]. The flow resistivity is measured by sending an air flow with constant velocity through the material, and measuring the air velocity and pressure drop across the sample [16]. The geometry of the test sample can be cylindrical or rectangular. The flow resistivity in the uni-directional sample is calculated as

$$\sigma = -\frac{\Delta p}{V \cdot t}, \tag{3.9}$$

which is essentially the same as Eq.(3.1), with $\Delta p = p_2 - p_1$, [2].

The test set-up used in the Marcus Wallenberg Laboratory (MWL) is depicted in Figure 3.4. It follows the set-up developed at the Acoustics Laboratory of the Université du Maine (LAUM), France. The geometry of the test samples is cylindrical, and is defined by the sample container. A pressure sensor SwemaMan 80 is used to estimate the flow rate passing through the laminar element Meriam 50MJ10-12 just before it enters the sample; the pressure drop across the tested sample is estimated using a differential pressure transmitter model FCO332 from Furness Controls. [9]

In order to prevent non-linear flow to develop, very small pressures and flow rates should be used. The International Standard ISO 9053 [11] prescribes flow rates between 0.5 and 4 mm/s. Exceeding the flow rate might affect the quality of the measurement. Other factors can also affect the quality of the measurement, e.g. imperfections in the preparation of the sample, or leakage of air in the measurement cell if the sample does not fit tight. [1]

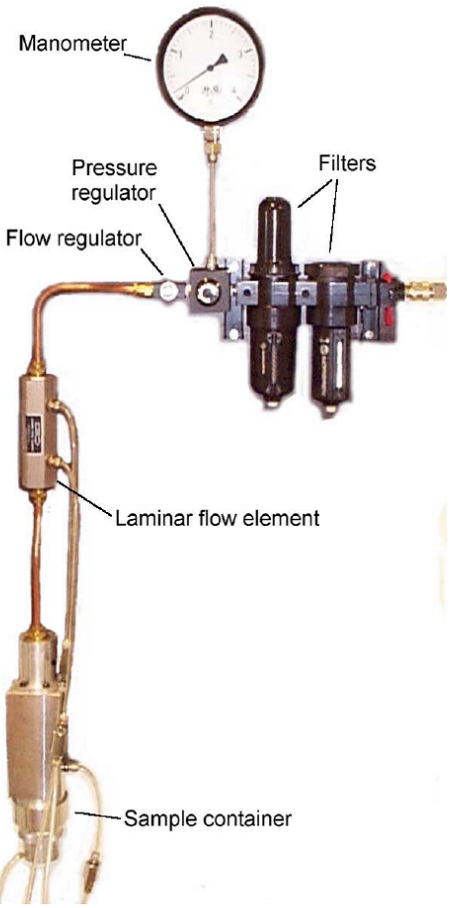

Figure 3.4: Set-up for measurement of flow resistivity in the MWL laboratory (Ahlquist [1]).

A significant deviation in the set-up in the MWL laboratory compared to the International Standard ISO 9053 [11] is that the diameter of the cylindrical measurement cell is 44 mm, instead of the specified minimum 95 mm. However, this deviation from the International Standard ISO 9053 [11] is believed to have a minor influence, as the results obtained with this device are in the same range as measurement results published by others for similar materials.

3.2.2 Observations about the International Standard ISO 9053

The International Standard ISO 9053 [11] is limited to the measurement of uni-directional samples, which would be sufficient if all porous materials were homogeneous and isotropic. However, due to the production processes involved (see chapter 2), porous materials are rarely isotropic and homogeneous, at least not at a reasonable production cost. Having access to uni-directional measurement data only may, under certain circumstances, create difficulties for proper characterisation of a highly anisotropic material. Three examples of such circumstances are given here.

Misalignment of measurement direction and principal direction of the material.

An orthotropic material has three principal directions along which the flow resistivity is described by one value, the corresponding principal value (see Eq.(3.7)). If the principal directions of the material are known, the cylindrical sample may be extracted so that the axis of the sample coincides with one of the principal directions (see Figure 3.5a). In this case, the flow resistivity in the sample will be equal to one of the principal values (σ_1, σ_2 or σ_3, see Eq.(3.7)), and this value can be measured with the International Standard ISO 9053 [11]. If the axis of the cylindrical sample does not coincide with one of the principal directions (see Figure 3.5b), the flow resistivity measured in the sample will depend on all three principal values. This leads to inaccuracies in the measured flow resistivity, and might lead to non-optimal use of the material, and its properties, in critical applications.

Determination of flow resistivity in all directions in one point of the material.

The International Standard ISO 9053 [11] measures the flow resistivity in a *uni-directional* sample of material. Thus, it cannot measure the flow resistivity in more than one direction in one point of the material. In order to have information on all three principal flow resistivity values in the material, three different samples need to be measured in the three different main directions. This entails some additional uncertainties related to the homogeneity, local and global. If the material is not homogeneous over the area from which the three different samples are extracted, the measured flow resistivity value at the sample location might not be representative for the flow resistivity at other locations in the material. This also has the potential of leading to inaccuracies in the measured flow resistivity, and corresponding problems with non-optimal use. Furthermore, it would be

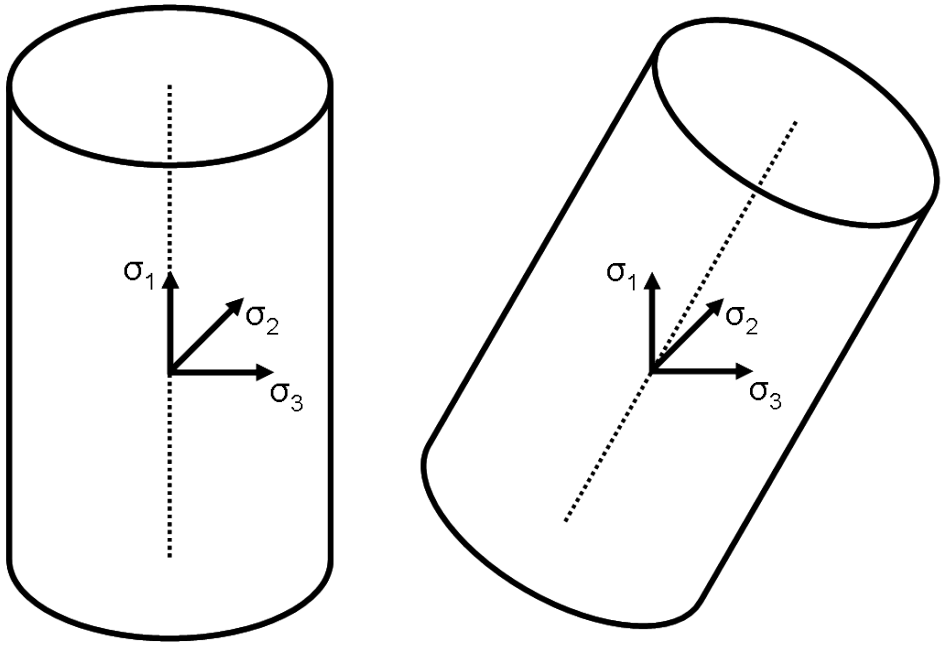

(a) Cylinder axis and principal axis aligned

(b) Cylinder axis and principal axis not aligned

Figure 3.5: Misalignment of measurement direction and principal direction of material. The dotted line gives the axis of the cylinder.

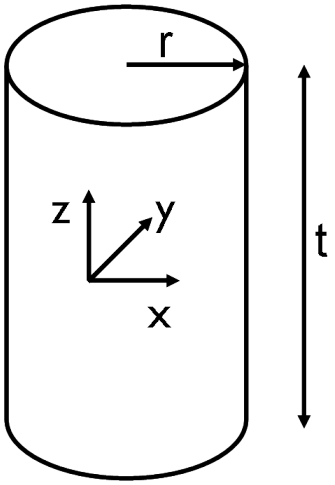

Figure 3.6: Orientation of the axes in the cylindrical sample.

much more accurate and efficient, if all three principal values and corresponding principal directions could be deduced with only one sample.

Determination of flow resistivity in a thin sample.

The International Standard ISO 9053 [11] defines a requirement for the minimum lateral dimension (diameter for a cylindrical cross-section or side for a rectangular cross-section) of the test specimen. The only requirement concerning the thickness of the specimen is that "The thickness of the test specimen shall be chosen to obtain pressure drops measurable under optimum conditions, and to suit the usable depth of the measurement cell" [11]. It neglects the effect on the measured flow resistivity related to the thickness of the specimen, a fact that could be critical in the case of an anisotropic material sample.

This latter point may be illustrated by considering a cylindrical sample of an anisotropic material with thickness t and radius r. The axis system is defined as shown in Figure 3.6. For a sample with a thickness much smaller than the diameter ($t << r$), it is shown in paper **B**, section 3.1.1, that the measured flow resistivity equals

$$\sigma_{thin} = \sigma_{zz} - (\frac{\sigma_{yy}\sigma_{xz}^2 + \sigma_{xx}\sigma_{yz}^2 - 2\sigma_{xz}\sigma_{xy}\sigma_{yz}}{\sigma_{xx}\sigma_{yy} - \sigma_{xy}^2}). \tag{3.10}$$

For a sample with a thickness much larger than the diameter ($t >> r$), it is shown in paper **B**, section 3.1.2, that the measured flow resistivity is

$$\sigma_{thick} = \sigma_{zz}. \tag{3.11}$$

These expressions are verified by performing simulations on a Finite Element (FE) model, and the result of the verification can be found in paper **B**, section 3.2. For anisotropic

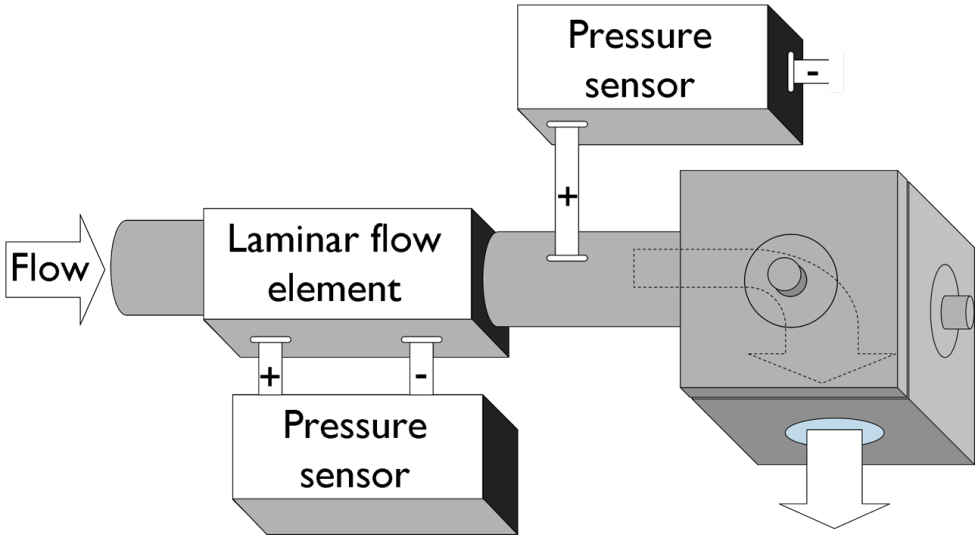

Figure 3.7: General arrangement of the measurement set-up.

materials for which the flow resistivity is not measured along a principal direction (which already gives an underestimation of the flow resistivity), measuring a thin sample might lead to an additional underestimation of the flow resistivity of the material.

Closing remark on the measurement of flow resistivity with the International Standard ISO 9053.

The present state-of-the-art porous materials are in most cases both anisotropic and inhomogeneous, as a result of the production processes involved. The measurement method for flow resistivity, defined by the International Standard ISO 9053 [11], does not give sufficient knowledge for a proper characterisation of a highly anisotropic material. Consequently, an alternative method has to be considered which identifies the full *anisotropic* flow resistivity tensor, and which makes it possible to estimate the principal values and principal directions of flow resistivity for *each* point in a material.

3.2.3 Method to identify the full anisotropic flow resistivity tensor of porous materials

In the previous section, it was pointed out that there is a need for a more accurate and omni-directional method to estimate the flow resistivity in porous materials. Göransson et al. proposed an alternative method [9] in which the full anisotropic flow resistivity tensor is estimated. The method, consisting of measurements and subsequent inverse estimation, is described with more details in section 3 of paper **A**, and is briefly summarised here.

The measurement set-up can be seen as a generalisation of the standardised 'static flow - pressure drop' measurement set-up. A cubic measurement cell with openings on all sides replaces the uni-directional measurement cell. Figure 3.7 shows the general arrangement of the measurement set-up. In the approach used, the pressure differences across the sample are measured in all possible flow directions. The flow resistivity tensor is identified by inverse estimation, in which the governing equation is based on Darcy's law [6], assuming that the flow is incompressible. A possible solution for the flow resistivity tensor is inserted in a FE model with appropriate boundary conditions, and the pressure differences across this modelled sample are calculated in all possible flow directions. The differences between the measured and calculated pressure differences is then minimised in the least square sense, using the optimiser Globally Convergent Method of Moving Asymptotes (GCMMA) [15].

This latter aspect deserves some additional attention. The optimisation process used in the original method [9] is the optimisation algorithm Method of Moving Asymptotes (MMA) by Svanberg [14]. With this algorithm, convergence is not fully assured, as the proposed set of parameters does not necessarily respect the constraints. The GCMMA optimiser is an updated version of the MMA optimiser, and has an internal iteration loop that checks if the approximation proposed by the optimiser gives a conservative estimation of the solution, i.e., not worse than the previous solution.

In paper **A**, section 4.1, a comparison between both optimisers shows that a satisfactory accuracy can be reached with the MMA optimiser after a total of 10500 FE calculations (calculation time $\approx$ 23h), while the GCMMA optimiser requires 9300 FE calculations (calculation time $\approx$ 21h) to obtain a solution with the same accuracy. The effect of the internal iteration loop in GCMMA can be seen in Figure 3.8 (Figure 3c in paper **A**). The figure shows how a flow resistivity value is found with both the MMA and the GCMMA optimiser. The graph representing the GCMMA optimiser increases monotonically towards the target value (2800) while the graph for the MMA optimiser fluctuates around the target value.

In the paper describing the original method [9], a successful verification of the repeatability and robustness of the method is reported. In addition, the estimation procedure was verified for a theoretical transversely isotropic material. The generality of the approach may be extended to orthotropic materials, and this is investigated in section 4 in paper **A**. Four artificial orthotropic flow resistivity tensors are set as a target for the inverse estimation, and are found with very good accuracy, showing the validity of the approach.

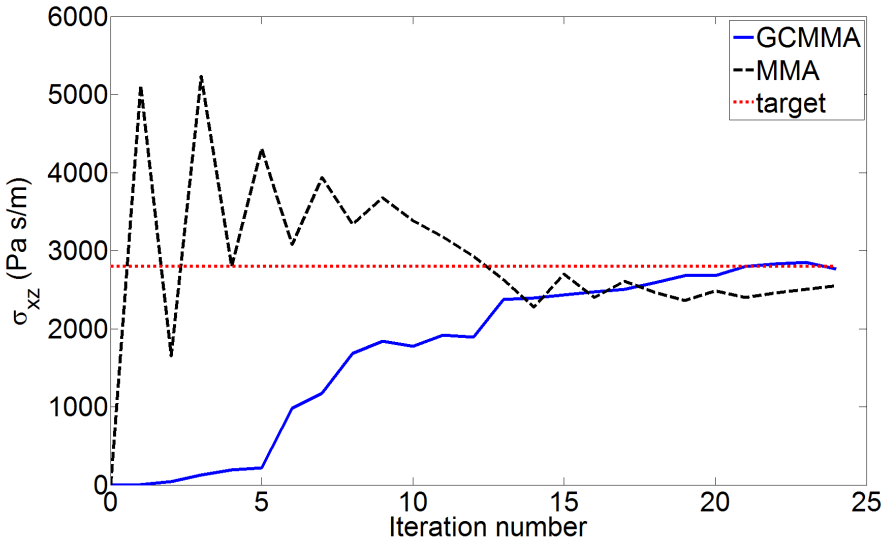

Figure 3.8: Retrieving an artificial flow resistivity value set as target in the verification of the method.

Chapter 4

Inverse estimation of flow resistivity in Melamine foam and glass wool

In this chapter, the alternative method with measurement and inverse estimation is applied to glass wool and Melamine foam samples. The two materials are expected to exhibit different degrees of anisotropy in the flow resistivity. The objective of identifying the flow resistivity tensor in glass wool is to verify the hypothesis concerning the transverse isotropy in the material, and to study the variations in a slab of glass wool material. The objective of identifying the flow resistivity tensor of Melamine is to gain insight into the characterisation of the anisotropy in a non-layered material.

4.1 Description of the materials tested

4.1.1 Glass wool

Chapter 2 discussed the production process of glass wool, and its characteristic anisotropy caused by the production process. Glass wool has a rather low degree of anisotropy, with respect to flow resistivity, which is linked to the layering of the fibres, and the subsequent compression to desired thickness and density [9]. The material tested in this study is expected to exhibit a clear transverse isotropy.

The method for 3D identification of flow resistivity is applied to nine glass wool samples that are extracted from a slab of glass wool delivered by Ecophon. The slab measured 1200 x 600 x 100 mm^3, and the average density of the glass wool samples is estimated to be 27.8 kg/m^3. Cubic samples suited for measuring are extracted from the middle of the slab, as shown in Figure 4.1. The porosity of the samples is estimated to be 0.99.

The directions in the glass wool are described by a rectangular coordinate system. The x and y axes are chosen to be in the plane of layers, while the z axis is chosen to be

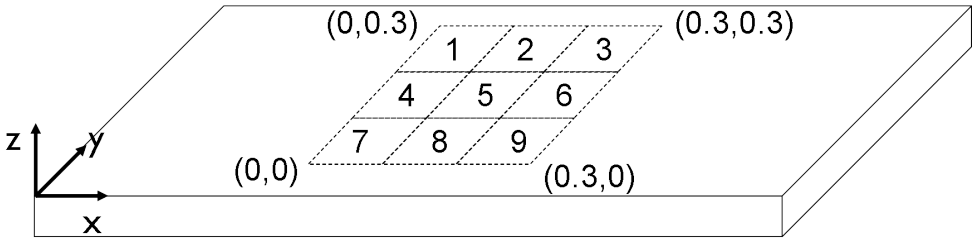

Figure 4.1: Spatial arrangement of all nine samples in the larger slab.

in the stacking direction, perpendicular to the plane of layers. This coordinate system applies to each of the extracted samples.

4.1.2 Melamine foam

In chapter 2, it is pointed out that Melamine foam exhibits a characteristic anisotropy related to the influence of gravity during expansion of the foam, in combination with the placement of the injection nozzles, depending on the production processes involved. However, little is known on the degree of anisotropy in the Melamine foam tested, as there is not much information available about the production process. No information is known on the placement of the nozzles, nor the exact manufacturing process itself. Only the rise direction in which the foam blocks are grown is known to the author.

The 3D flow resistivity identification method is applied to seven different Melamine samples. Cubic samples suited for measuring are extracted from the corner of two larger blocks of foam. The location of the extracted samples with respect to each block is depicted in Figure 4.2. The average density of the samples is 9.2 kg/m^3, and the porosity of the samples is estimated to be 0.99.

The directions in the Melamine foam are described by a rectangular coordinate system. Samples 1 to 4 have the rise direction in-plane, i.e., perpendicular to the z axis. Samples 5 to 8 have the rise direction parallel to the z axis.

4.2 Flow resistivity tensors of glass wool and Melamine foam

The anisotropic flow resistivity tensors depend on the orientation of the samples, and the inherent directionality induced by the applied production processes. The eigenvalue and eigenvector decomposition of the tensor is considered to be more valuable, as it gives

(a) Melamine samples 1 to 4 -
rise direction in-plane, $\perp z$ axis

(b) Melamine samples 5 to 8 -
rise direction out-of-plane, $\parallel z$ axis

Figure 4.2: Position of extracted Melamine samples 1 to 8 from larger blocks of Melamine foam.

a better understanding of the intrinsic flow resistivity of the materials. Moreover, it provides a clearer view of the characteristic anisotropy of the material, as the tensor is transformed to Eqs.(3.6), (3.7), or (3.8), and the principal directions and principal values in the material may be extracted.

Table 4.1 presents a summary of the identified anisotropic flow resistivity tensors. The detailed flow resistivity tensors may be found in Table 4 in paper **A** for Melamine foam, and in Table 2 in paper **B** for glass wool. As the principal direction for each sample is aligned with the imposed axis system, the axis that is parallel to the principal direction corresponding to each principal value is given, along with the principal value and the residue of the cost function.

Table 4.1: Summary of the identified anisotropic flow resistivity tensors.

	Glass wool		Melamine foam	
Sample number	Eigenvalues & directionality	Residue	Eigenvalues & directionality	Residue
1	$\sigma_1 = 6700 \rightarrow y$ $\sigma_2 = 7000 \rightarrow x$ $\boldsymbol{\sigma_3 = 8800 \rightarrow z}$	0.050	$\sigma_1 = 9200 \rightarrow z$ $\sigma_2 = 9300 \rightarrow y$ $\boldsymbol{\sigma_3 = 9800 \rightarrow x}$	0.022
2	$\sigma_1 = 7000 \rightarrow y$ $\sigma_2 = 7400 \rightarrow x$ $\boldsymbol{\sigma_3 = 10300 \rightarrow z}$	0.082	$\sigma_1 = 9900 \rightarrow z$ $\sigma_2 = 10100 \rightarrow x$ $\boldsymbol{\sigma_3 = 10300 \rightarrow y}$	0.040
3	$\sigma_1 = 7200 \rightarrow y$ $\sigma_2 = 7600 \rightarrow x$ $\boldsymbol{\sigma_3 = 9300 \rightarrow z}$	0.19	$\sigma_1 = 10300 \rightarrow z$ $\sigma_2 = 10800 \rightarrow y$ $\boldsymbol{\sigma_3 = 11000 \rightarrow x}$	0.020
4	$\sigma_1 = 6500 \rightarrow y$ $\sigma_2 = 6700 \rightarrow x$ $\boldsymbol{\sigma_3 = 8900 \rightarrow z}$	0.071	$\sigma_1 = 10100 \rightarrow z$ $\sigma_2 = 11000 \rightarrow x$ $\boldsymbol{\sigma_3 = 11300 \rightarrow y}$	0.016
5	$\sigma_1 = 6200 \rightarrow x$ $\sigma_2 = 6700 \rightarrow y$ $\boldsymbol{\sigma_3 = 9200 \rightarrow z}$	0.090	$\sigma_1 = 10100 \rightarrow x$ $\sigma_2 = 10800 \rightarrow y$ $\boldsymbol{\sigma_3 = 11500 \rightarrow z}$	0.016
6	$\sigma_1 = 6400 \rightarrow x$ $\sigma_2 = 6900 \rightarrow y$ $\boldsymbol{\sigma_3 = 9800 \rightarrow z}$	0.036	$\sigma_1 = 9700 \rightarrow y$ $\sigma_2 = 9800 \rightarrow x$ $\boldsymbol{\sigma_3 = 10900 \rightarrow z}$	0.030
7	$\sigma_1 = 6200 \rightarrow x$ $\sigma_2 = 6600 \rightarrow y$ $\boldsymbol{\sigma_3 = 7100 \rightarrow z}$	0.19	$\sigma_1 = 9800 \rightarrow x$ $\sigma_2 = 10600 \rightarrow y$ $\boldsymbol{\sigma_3 = 11100 \rightarrow z}$	0.035
8	$\sigma_1 = 6500 \rightarrow y$ $\sigma_2 = 6900 \rightarrow x$ $\boldsymbol{\sigma_3 = 8600 \rightarrow z}$	0.039		
9	$\sigma_1 = 6800 \rightarrow x$ $\sigma_2 = 7000 \rightarrow y$ $\boldsymbol{\sigma_3 = 8000 \rightarrow z}$	0.14		

4.2.1 Glass wool

In glass wool, the principal direction of highest flow resistivity is in all samples parallel to the stacking direction. This was expected, since it should be easier for the air to flow parallel to the layers than to move through to the layers. All samples are close to transverse isotropic, as the difference $(\sigma_1 - \sigma_2)$ between the in-plane principal values is small, compared to these values. The transverse isotropy may also be shown by calculating the ratio of out-of-plane over in-plane flow resistivity. The average in-plane

flow resistivity (calculated as the average of σ_1 and σ_2) equals 6800 Pa·s/m^2; the average out-of-plane flow resistivity (calculated as the average of σ_3) is 8900 Pa·s/m^2. This gives an average ratio of out-of-plane vs. in-plane flow resistivity equal to 0.76. This is closer to the theoretical value found by Tarnow (0.67) [16], than to the values measured by Allard (0.6) [3] and Göransson (0.57) [9].

The residue of the cost function is in most of the cases small apart from 3 samples where it is higher. This might be due to irregularities in the material, as glass wool is not always a perfectly layered material. Sometimes sublayers may be deformed, creating pockets, and lumps of resin and fibres. Locally in the sample, this might result in a higher or lower bulk density, and can have an effect on the flow resistivity, as it reflects the number of fibres present in a given volume of material.

Together with the average in-plane and out-of-plane flow resistivity, the standard deviation can be calculated. The standard deviation for in-plane flow resistivity is 300 Pa·s/m^2 (average of 6800 Pa·s/m^2), and the standard deviation for out-of-plane flow resistivity is 900 Pa·s/m^2 (average of 8900 Pa·s/m^2). This results in a large spread on the estimated out-of-plane flow resistivity up to 32%, and can be attributed to the low bulk stiffness of glass wool in the stacking direction. Therefore, it is easily deformable in this direction, which might result in the creation of pockets, local distortions in the fibre arrangements, or in layers moving closer towards each other, as shown in Figure 4.3. The bulk stiffness in the plane of layers is much higher (up till 50 times [16]), and hence the in-plane flow resistivity varies less, up to 15%. Nevertheless, the in-plane flow resistivity is as well influenced by local distortions in the material.

4.2.2 Melamine foam

It is interesting to see from Table 4.1, in which the residue of the cost function is small for all cases, that the principal direction corresponding to the highest flow resistivity coincides with the rise direction of the samples tested. Some of the samples tested seem to be transversely isotropic, which may be related to the rise direction. However, some samples seem to be closer to isotropy, and others to orthotropy. From the results in Table 4.1, it is hard to draw general conclusions concerning the anisotropy of the flow resistivity in the material, other than the obvious fact that the direction of highest flow resistivity is aligned with the rise direction.

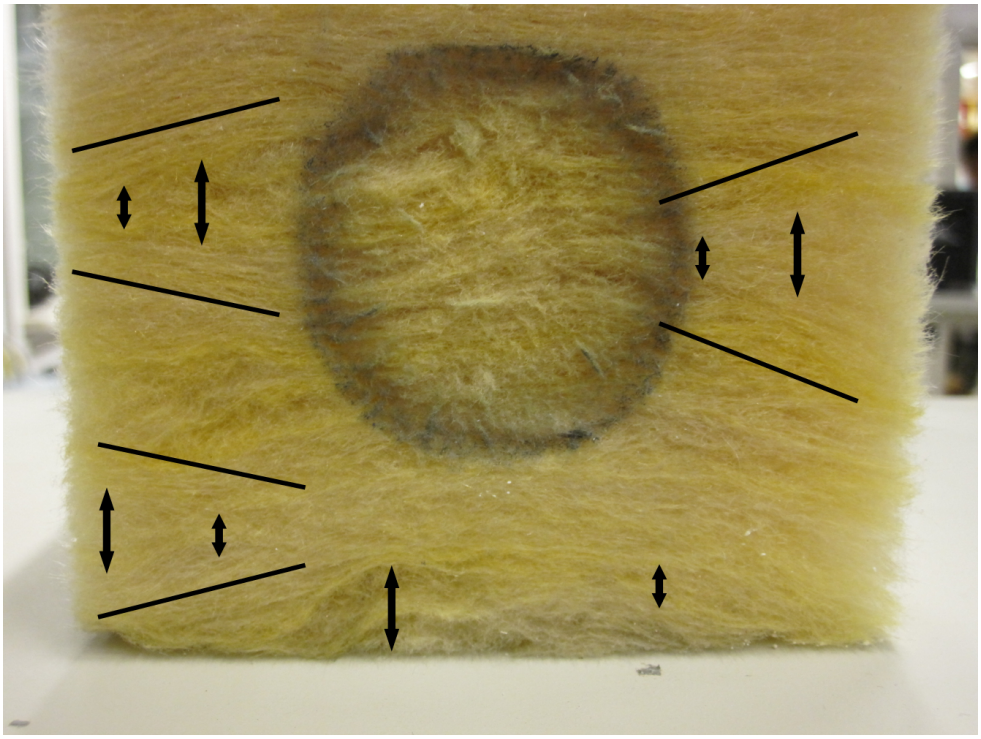

Figure 4.3: Distortions in glass wool sample.

4.3 Validation of the estimated flow resistivity tensors

In order to validate the estimated flow resistivity tensors obtained by the inverse estimation, cylindrical samples are extracted from the tested cubic samples. The flow resistivity in these cylindrical samples is measured with the measurement set-up in the MWL laboratory, shown in Figure 3.4. To make a valid comparison between the uni-directional measurement and the estimated flow resistivity tensors, a cylindrical tube-like FE model represents the uni-directional measurement, and the estimated flow resistivity tensor is inserted in the FE model to calculate the corresponding uni-directional flow resistivity.

Table 4.2 presents a summary of the validation of the estimated anisotropic flow resistivity tensors. The details of the validation can be found in section 6 in paper **A** for Melamine foam, and in section 5 in paper **B** for glass wool.

Differences between the measured and FE computed flow resistivity can have three causes. Measurement errors and sample preparation, the inverse estimation, or the local distortions in the material can all contribute in various degrees to the differences.

Table 4.2: Validation of estimated flow resistivity tensors.

	Glass wool		Melamine foam	
Coordinate direction	Uni-directional FE computation	Uni-directional measurement	Uni-directional FE computation	Uni-directional measurement
X	7400 6400 6200	6200 5700 5200	10100	9500 9200 10800 10300
Y	7400 6500 6500	6200 5600 6000	9300	9400 8800
Z	8800 9200 8000	9500 10300 9400	10300	9800 9800 10000 9900

For the 3D identification method, the inverse estimation has been successfully verified, and the sample preparation has a minimal effect on the flow resistivity of the material, as the samples are cut with a very thin saw. The measurement errors in the cubic measurement set-up are rather small, since for every direction in which the pressure difference is measured, there is a reciprocal direction which is used as quality control check. If the deviation is larger than 5% between reciprocal directions, the measurement is not accepted. Therefore, it is most likely that local distortions in the material are responsible for deviating results.

In the uni-directional measurements, the samples are extracted with a hollow punch attached to rotating drilling machine. The punch pushes/rotates through the material, and this can affect the flow resistivity considerably. Besides the sample preparation, also local distortions in the material yield part of the difference, and might be more outspoken in the cylindrical samples than in the cubic samples, since the volume of tested material is smaller.

4.3.1 Glass wool

The maximum relative error between measured and FE computed flow resistivity is 18%. This is a considerable difference that can be explained by examining the bulk stiffness of the material and the sample preparation. The bulk stiffness of glass wool in the stacking direction is up till 50 times lower than the bulk stiffness in the in-plane direction [16]. Therefore, the cylindrical samples extracted from glass wool in the stacking direction are more influenced by the compressions caused by the extraction method, and by the

mounting of the sample in the measurement cell. If a material is compressed, it is expected to have a higher flow resistivity. The other directions in glass wool are as well influenced by the layered structure. The higher in-plane bulk stiffness, which is a consequence of the layered structure, makes it difficult to extract a cylindrical sample in the plane of layers, causing damages to the sample, which might lower the flow resistivity measured in the sample. This might explain why the measured flow resistivity in the stacking direction, in all uni-directional samples, is higher than the FE computed flow resistivity, and why the opposite is true for the in-plane directions.

4.3.2 Melamine foam

The maximum relative error between measured and FE calculated flow resistivity is 9%, which is a satisfying result. The difference may also here be attributed to measurement errors, inaccuracies in the inverse estimation method or irregularities in the material. However, the differences are much smaller than for glass wool, since Melamine foam is not affected by the properties induced by a layered structure. Melamine foam does not exhibit such a large difference in bulk stiffness between the rise-direction and other directions. Nevertheless, the small compression as a result of the extraction and mounting of the sample can still have a (less pronounced) influence on the measured flow resistivity. Other causes of the difference might be local effects in the extracted cylindrical samples. It seems that these local effects can be more important than the effect of the compressions, unlike in glass wool. As an example, sample 2 in Table 5 (in paper **A**) seems to be affected by local effects in the cylindrical samples, as there is a large variation in flow resistivity in this cubic sample.

4.4 Surface map of the flow resistivity in glass wool

As data was obtained of nine samples, this allowed for calculating a surface map of the flow resistivity over the whole slab. This was done for the in-plane (Figure 4.4) and out-of-plane flow resistivity (Figure 4.5). The estimated in-plane and out-of-plane flow resistivity values from Table 4.1 are assigned to the middle of each sample, and a surface, which approximates the data, was estimated on the 2D grid. The figures show that the flow resistivity varies considerably in the material. In most of the material the out-of-plane flow resistivity is higher than the in-plane flow resistivity. However, at the (0,0) coordinate the estimated in-plane flow resistivity is larger than the estimated out-of-plane flow resistivity, which is unexpected, and can probably be attributed to local distortions in the cubic sample number 7, in which the flow resistivity in stacking direction is rather low.

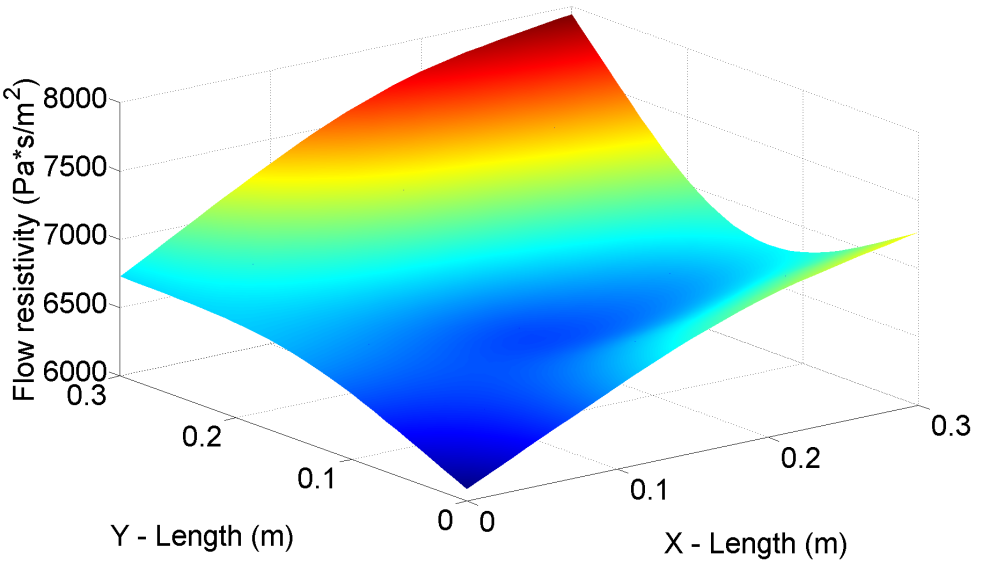

Figure 4.4: Estimation of the variation of the in-plane flow resistivity in glass wool.

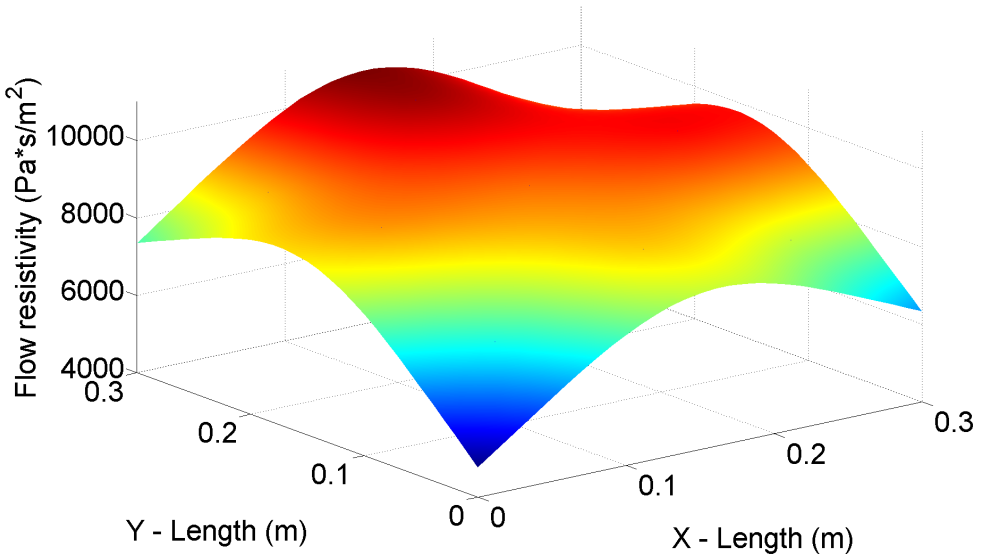

Figure 4.5: Estimation of the variation of the out-of-plane flow resistivity in glass wool.

4.5 Comparison of variation of flow resistivity and density

The flow resistivity is not uniform in a block of material. This may be concluded from Tables 4 and 5 in paper **A**, and from Tables 2 and 3 in paper **B**. These tables show that neither is the density uniform in the slab of material. It is interesting to investigate if there is a relation between the variation in flow resistivity and density.

This relation is possible, since the manufacturers of the materials most likely try to obtain a certain target value for the material properties during the production process. The properties of Melamine foam can be influenced by the composition of the injected solution, the curing process, the foaming process, the shape of the foaming chamber, the positions of the injection nozzles, and other processes involved. The properties of glass wool can be influenced by controlling the fibre radius, the thermosetting, or the compression of the material.

Thus, it could be expected that the manufacturing processes influence the density and the flow resistivity of the material. Consequently it is possible that there is a relation between the targeted flow resistivity and density on the scale of the block of material. Homogeneity is assumed in the material block as a final product, and the material properties are considered uniform. However, inhomogeneities at micro level can propagate into the material properties at macro level. For this reason, there might still be variations in the material properties, variations which are small compared to the values targeted in the production process. In the Melamine foam and glass wool tested in the course of this work, there seems to be no relation between the variation in flow resistivity and density. This means that the properties are variating independently from each other, although they are both believed to be caused by inhomogeneities at micro scale.

In *Melamine foam*, a local increase in material density could indicate the presence of a larger amount of solid material per unit volume. This can happen if the struts on microscopic level are thicker, or if there are more struts (of the same thickness) per unit volume. This could possibly correspond to a local increase in flow resistivity. However, a local increase in density does not necessarily lead to an increase in the flow resistivity. An increase in density can also occur, if a volume with 4 struts of equal thickness is replaced by a volume containing 1 strut which is 4 times as thick as one of the other struts. The density would then locally increase by a factor 4. However, the volume with this one thick strut will offer less resistance to the flow than a volume with the 4 thin struts. A comparison with trees can easily be made. To stop the wind from blowing through the garden, it seems wiser to put 4 thinner trees next to each other instead of just one big tree.

For *glass wool*, a surface map of the density is estimated and plotted in Figure 4.6. A

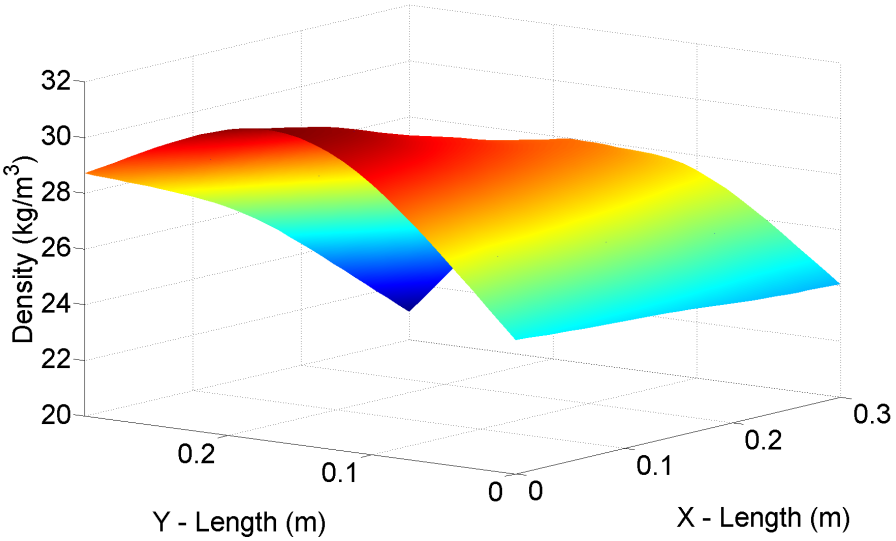

Figure 4.6: Estimation of the variation of the density in glass wool.

comparison between the surface maps for density and flow resistivity shows no relation on this scale between both properties. Local effects in the material might, also in this case, influence the variation of both flow resistivity and density in an uncontrolled way. In glass wool, the radius of the fibres is shown to vary considerably around an average value (e.g. average fibre radius of 3.4 μm and standard deviation of 1.3 μm [16]), fibres might cling together in pairs, and in some parts of the material the layers might be more compressed than in others. All these local effects can occur in the final product, and influence the flow resistivity and density independently from each other.

4.6 Closing remarks on the used inverse estimation method

It may be concluded that the alternative method to identify the full flow resistivity tensor of porous materials works. One reason to conclude this are the, in general, small cost function residues that remain at the end of the optimisation process. In some cases the residues are larger, but they are believed to be material or measurement dependent, rather than artefacts of the method. The repeatability and the robustness of the method were discussed in [9], and found to be satisfactory. In paper **A** the computational part of the method is verified, and found to correctly estimate the flow resistivity tensor of porous materials.

There are still some details about the method that need further investigations. An interesting observation for most of the samples studied, is that all principal directions are aligned with the imposed coordinate axes (see Table 4 in paper **A** and Table 2 in paper **B**). In the inverse estimation, the terms that are sought are the six unknown terms in the flow resistivity tensor. Another approach would be to estimate the principal values and directions. From the six terms to be estimated, the three diagonal terms are identified quickly with good accuracy. It takes more time to identify the three off-diagonal values, and the convergence appears to be dependent on the chosen starting values, whereas the diagonal values are not at all sensitive to the starting values chosen. This is possible if the influence of the off-diagonal terms is really small, which is the case if all samples are prepared in such a way that the imposed axes are aligned with the principal directions. For glass wool this is intelligible, since the stacking direction of the material is known, and the material is generally assumed to behave transversely isotopic in terms of flow resistivity. However, little is known about the Melamine samples, and it might be a coincidence that the principal directions are aligned with the imposed axes. Therefore it would be interesting to perform tests on a material sample which is known to have principal directions that do not coincide with the imposed axes. It was tried to 'fake' such a material in the verification of the method, by using tensors which have smaller and larger off-diagonal terms to see if they are retrieved correctly. In all cases of the verification, the a priori known tensors were found (section 4 in paper **A**). Thus, the inverse estimation does not implicitly favour the diagonal terms in the estimation, i.e., the relative errors in the cost-function for the optimisation are not weighed in any way so that the diagonal terms would be found with better accuracy.

Figure 4.7 shows a second detail that needs further investigation. It is an inconsistency in the computational part of the method. When the inverse estimation is repeated for the same measurement data, using the exact same inputs, and leaving all parameters in the inverse estimation unchanged, it has been observed that the convergence history (and the solution) for both inverse estimations was slightly different. The FE model gives a different output in one of the iterations in the inverse estimation, which has an influence on the rest of the inverse estimation. The problem might most likely be related to the mesh in the FE model. The initial mesh is a 'normal' mesh, and while solving the problem, one adaptive mesh is necessary to approximate the solution at the sharp edges of the model (see Figure 2 in paper **A**). This meshing procedure (normal mesh and one adaptive mesh) is found to be optimal to avoid corrupted elements in the mesh. However, the adaptive meshing is based on a random algorithm, and thus the mesh might slightly differ in every model, which affects the FE output. The solutions usually do not differ much, as a result of the optimisation process. An algorithm which limits the output of the FE calculations to seven significant digits has been successfully implemented as a workaround, to minimise the effect of the random factor in the adaptive meshing. A permanent solution is not to use the adaptive mesh, e.g. by implementing a manual

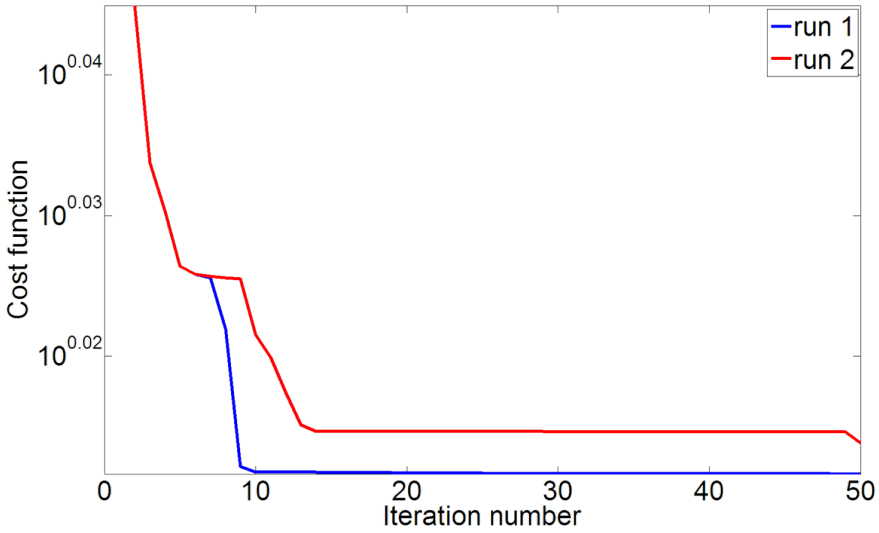

Figure 4.7: The adaptive meshing in COMSOL Multiphysics leading to a difference in solution for same inputs.

mesh-handling procedure.

Chapter 5

Conclusions and Future work

This thesis discusses the determination of the anisotropic flow resistivity tensor in Melamine foam and glass wool. There is a need for an alternative method to measure the flow resistivity in anisotropic materials, as the uni-directional measurement described by the International Standard ISO 9053 [11] seems to be insufficient to provide flow resistivity data that allow for a proper characterisation of anisotropic materials.

The inverse estimation method for identification of the full anisotropic flow resistivity tensor, which was originally developed by Göransson et al. [9], has been improved and verified.

- The GCMMA optimiser is an improvement, since it assures a converging solution, and reaches a satisfactory solution in less iterations than the MMA optimiser.
- The computational part of the method is successfully verified by setting artificial and a priori known orthotropic tensors as target for the inverse estimation.
- The overall approach of the method is validated by comparing the estimated flow resistivity tensors to cylindrical samples extracted from the cubic samples tested.

These results are very important as they show that the approach with inverse estimation works, when identifying the flow resistivity for anisotropic materials.

In glass wool, inspecting the eigenvalue and eigenvector decomposition of the estimated flow resistivity tensors, showed that the flow resistivity is transverse isotropic in all samples. This was expected, since the material fibres are oriented in layers, which are stacked together. The findings in this work that the transverse isotropy of glass wool involves a higher flow resistivity in the stacking direction, confirms earlier conclusions by Tarnow [16], Allard [3], and Göransson [9].

In addition, for the glass wool, it was possible to extract nine adjacent samples from the same slab, and to investigate the variation of the density and flow resistivity in the material, based on the flow resistivity tensor identified for each sample. The results are illustrated by estimating a surface map for both flow resistivity and density of the glass wool. Both exhibit a large variation in the slab, especially the flow resistivity in the stacking direction, as the material is most easily deformed in this direction.

The anisotropy in Melamine foam, induced by the rise direction, and the highest flow resistivity in the rise direction of the material have not been shown before. This seems of great relevance for the acoustical application of Melamine foam. It is an important conclusion of this thesis, and further research might be able to link these findings to the micro-structural geometry of the materials, which might lead to similar conclusions related to the other macroscopic properties of Melamine foam.

An examination of the variation of flow resistivity and density in both materials seemed to show no relation between the density and flow resistivity in neither Melamine foam nor glass wool, based on the measurements done in this study. Possible causes are related to the inhomogeneities on micro scale, which might influence both material properties independently from each other.

Some issues concerning the inverse estimation, that are addressed throughout the thesis, still have to be solved, and another approach based on finding the principal values and principal directions of the flow resistivity tensor, in stead of all six unknown terms in the tensor, might improve the method. The application of the optimiser should as well be further improved, so that the optimisation process is independent of the range of the values to be estimated, and, moreover, the calculation time should be reduced. Once these smaller changes have been introduced, it would be interesting to do independent inter-laboratory measurements to examine the precision of the method. Research challenges such as relating the micro-structural geometrical variation in a material to the anisotropic flow resistivity could then also be addressed in more depth.

The work described in this thesis has focused on estimating one parameter that is important for the acoustic performance of porous materials. Future work will concentrate on the other parameters to be estimated such as the elastic and dynamic moduli. Measurements have been done with respect to the characterisation of these properties, and the development of the inverse estimation is ongoing.

References

[1] J.R. Ahlquist. Porous foam characterization and simulation. Master's thesis, KTH, Stockholm, 2001.

[2] J.F. Allard and N. Atalla. *Propagation of Sound in Porous Media: Modelling Sound Absorbing Materials*. Wiley, second edition, 2009.

[3] J.F. Allard, R. Bourdier, and A. L'Esperance. Anisotropic effect in glass wool on normal impedance in oblique incidence. *Journal of Sound and Vibration*, 114:233–238, 1987.

[4] H. Baumgartl, B. Gross, and J. Schierholz. Shaped articles of melamine/formaldehyde foams having low formaldehyde emission, patent 7714031, May 2010.

[5] R.L. Brown and R.H. Bolt. The measurement of flow resistance of porous acoustic materials. *Journal of the Acoustical Society of America*, 13:337–344, 1942.

[6] H. Darcy. *Fontaines Publiques de La Ville de Dijon*. Libraire des Corps, 1856.

[7] L.J. Gibson and M.F. Ashby. *Cellular Solids: Structure and Properties*. Cambridge University Press, second edition, 1999.

[8] P. Göransson. *Numerical Modelling of Dynamics of Light Porous Materials*. PhD thesis, LTH, Lund, 1998.

[9] P. Göransson, R. Guastavino, and N. E. Hörlin. Measurement and inverse estimation of 3D anisotropic flow resistivity for porous materials. *Journal of Sound and Vibration*, 327:354–367, 2009.

[10] R. Guastavino. *Elastic and Acoustic Characterisation of Anisotropic Porous Materials*. PhD thesis, KTH, Stockholm, 2009.

[11] ISO 9053:1991: Acoustics – materials for acoustical applications – determination of airflow resistance, 1991.

[12] R.M. Jones. *Mechanics of Composite Materials*. Taylor & Francis, second edition, 1999.

[13] V. Schadler, M. Fricke, C. du Fresne von Hohenesche, and J. Roser. Porous material with a nonoporous coating, patent application 20090283480, November 2009.

[14] K. Svanberg. The method of moving asymptotes - a new method for structural optimization. *International Journal for Numerical methods in Engineering*, 24:359–373, 1987.

[15] K. Svanberg. A class of globally convergent optimization methods based on conservative convex separable approximations. *SIAM Journal of Optimization*, 12:555–573, 2002.

[16] V. Tarnow. Measured anisotropic air flow resistivity and sound attenuation of glass wool. *Journal of the Acoustical Society of America*, 111:2735–2739, 2002.

[17] Basf plasticsportal - foams - basotect. http://www.basotect.com, February 2011.

[18] European insulation manufacturers association. http://www.eurima.org, February 2011.

[19] Glossary of plastic injection molding terms. http://www.apisolution.com/images/glossary_plastic_injection_molding_engineering_manufacturing.pdf, February 2011.

[20] The university of dublin - trinity college. http://www.tcd.ie/Physics/Foams/solid.php, February 2011.